IEEJ TRANSACTIONS ON ELECTRICAL AND ELECTRONIC ENGINEERING
*IEEJ Trans* 2016; **11**: 5–9
Published online in Wiley Online Library (wileyonlinelibrary.com). DOI:10.1002/tee.22181

**Paper**

# Structural Change Induced in $LaAlO_3$ by Ion Implantation

Masayuki Harima*, Student member
Takaaki Morimoto*, Non-member
Yoshimichi Ohki*,**[a], Fellow

Ion implantation is used for various purposes in manufacturing semiconductor devices such as MOS-FETs. In the present study, the effects of implantation of $P^+$ or $B^+$ ions on the structural change of single-crystal $LaAlO_3$ were examined. The optical absorption edge located at ~5.6 eV, which seems to correspond to the bandgap energy of $LaAlO_3$, is hardly affected by the ion implantation. The X-ray diffraction peak intensity at $2\theta_\chi = 23.5^\circ$ is decreased by the ion implantation. The intensities of three sharp photoluminescence (PL) peaks detected at 1.62, 1.65, and 1.69 eV, which appear only when the samples are crystalline, become smaller by ion implantation. However, the intensity of a broad PL peak at ~2.8 eV due to the oxygen vacancy, which is detectable in both amorphous and crystalline samples, hardly changes after the ion implantation. These results indicate that the ion implantation degrades the crystallinity of $LaAlO_3$. © 2015 Institute of Electrical Engineers of Japan. Published by John Wiley & Sons, Inc.

**Keywords:** $LaAlO_3$, ion implantation, photoluminescence, X-ray diffraction, impurity, defect, oxygen vacancy

*Received 19 August 2014; Revised 9 December 2014*

## 1. Introduction

Ion implantation is widely used in various industries as a versatile method to provide various functions to many solid substances. For example, the authors have succeeded in giving the birefringence to silica glasses by the implantation of light ions, namely $H^+$ or $He^+$ [1–5]. By utilizing the birefringence, the authors have fabricated optical gratings, optical couplers, and polarization control elements. For the semiconductor industry, the most important use of ions is for the creation of donors and acceptors. Ion implantation through a gate dielectric to a Si substrate is also used for raising the threshold voltage of a metal–oxide semiconductor (MOS) device [6]. However, ion implantation inherently induces point defects, degradation of crystallinity, and appearance of localized electronic states in solids.

On the other hand, with the continued down scaling of MOS devices, $SiO_2$-based gate dielectrics have become even thinner, slated to reach >1 nm in the near future. It means that $SiO_2$ of this thickness would not act as an insulating layer, since direct tunneling dominates the leakage current. A possible solution is the use of high-permittivity (high-$k$) insulating layers [7]. For this purpose, zirconium-based or hafnium-based oxides have been investigated extensively [8–11]. Although hafnium-based oxides are being already used practically, they form silicates when they are on a Si substrate [12,13]. In this regard, lanthanum aluminate ($LaAlO_3$) is attracting much attention as a next promising gate insulator suitable for advanced MOS devices, because it has a high dielectric constant ($k$ ~25), a wide bandgap energy ($E_g = 5.6$ eV), and an atomic diffusion rate lower than that of hafnium-based oxides; also, it is thermally stable on Si [14]. Use of high-$k$ dielectrics is also anticipated in SiC power transistors such as MOSFETs and insulated-gate bipolar transistors (IGBTs) [15]. Since much higher voltage is applied to such devices than in the case of Si MOSFETs for large-scale integrations (LSIs), their gate dielectrics are thick, (e.g. 10–100 nm). This needs higher ion acceleration energies to pass through the dielectrics.

In manufacturing an MOS device, the threshold voltage of a device is often too low when it was manufactured. Therefore, in order to raise the threshold voltage to the designed value, ion implantation after the deposition of a gate dielectric is required [6]. However, as mentioned above, ion implantation may deform the crystal structure and induce defects in the dielectric. In this context, in the present study, we implanted ions into single-crystal $LaAlO_3$ and examined its effects by measuring the photoluminescence (PL), which is an effective tool for examining electronic localized states in various inorganic insulating materials [16], optical absorption to measure $E_g$, and X-ray diffraction (XRD) spectra to examine the crystal structure.

## 2. Samples and Experimental Procedure

Commercially available $LaAlO_3$ (100) single crystals grown by the Czochralski method were used as samples. They were of the shape of a plate with a thickness of 0.5 mm. Positive monovalent ions of phosphorus ($P^+$) or boron ($B^+$) were implanted into the samples with an acceleration energy of 100 keV at a dose of $1.0 \times 10^{15}$ $cm^{-2}$ using an ion accelerator (Ulvac, UP-150) at Waseda University. The reason for selecting 100 keV is that the present ion accelerator can work stably at this energy.

Before and after the ion implantation, PL measurements were carried out using synchrotron radiation (SR) as a photon source at the BL3B line of UVSOR Facility (Institute for Molecular Science, Okazaki, Japan, beam energy: 750 MeV). The beam line has a 2.5-m off-plane Eagle-type normal-incidence monochromator to disperse the radiation to monochromatic light. The PL spectrum, excited at each PL excitation peak energy, was measured with a 300-mm triple-grating monochromator (Acton, SpectraPro-300i) and a CCD camera (Princeton Instruments) at 10 K. The PL intensity was calibrated by taking into account the excitation SR intensity at each photon energy.

[a] Correspondence to: Yoshimichi Ohki. E-mail: yohki@waseda.jp

* Department of Electrical Engineering and Bioscience, Waseda University, Shinjuku, Tokyo 169-8555, Japan

** Research Institute for Materials Science and Technology, Waseda University, Shinjuku, Tokyo 169-8555, Japan

Optical absorption spectra were also obtained at room temperature using a Shimadzu UV-3100PC spectrometer equipped with deuterium and tungsten lamps as two photon sources. The spectrometer was also equipped with an integrating sphere attachment (ISR3100) to integrate the light coming from almost all the directions.

Furthermore, in-plane XRD spectra were obtained with Cu K$\alpha$ radiation at room temperature using a Rigaku Rint-Ultima III diffractometer in order to examine the change in crystallinity of the sample induced by ion implantation.

## 3. Results

Figure 1(a) and (b) show PL spectra observed at 10 K in photon energy ranges below and above 1.8 eV, respectively. Black solid curves are for the unimplanted samples, and the orange (light gray in b/w) ones are for the $P^+$-implanted samples, while the blue (dark gray in b/w) dashed curves are for the $B^+$-implanted samples. The dose of implanted ions was $10^{15}$ cm$^{-2}$ for each ion. From Fig. 1(a), the presence of three PLs excited by 6.0 eV photons at 1.62, 1.65 and 1.69 eV is confirmed. The intensities of the three PLs become weak by the ion implantation. On the other hand, it is confirmed from Fig. 1(b) that there is a very broad PL band spreading from ~1.8 to ~3.6 eV with a peak at ~2.8 eV. The intensity of this PL band shows almost no change by the ion implantation. Although the PL excitation spectrum is not shown, this PL showed the maximum intensity when it was excited by photons with an energy of ~5.0 eV.

Figure 2 shows the optical absorption spectra measured at room temperature before and after the implantation of $P^+$ and $B^+$ ions at a dose of $10^{15}$ cm$^{-2}$. It is known that $E_g$ of $LaAlO_3$ is ~5.6 eV [17]. From the spectra shown in Fig. 2, $E_g$, which can be estimated to have a similar value as the above, does not seem to be sensitive to the ion implantation. However, it is clearly seen that ion implantation decreases the absorption of photons with energies from 5.8 to 6.2 eV, which are slightly higher than $E_g$. The reason for this apparently strange phenomenon is unknown.

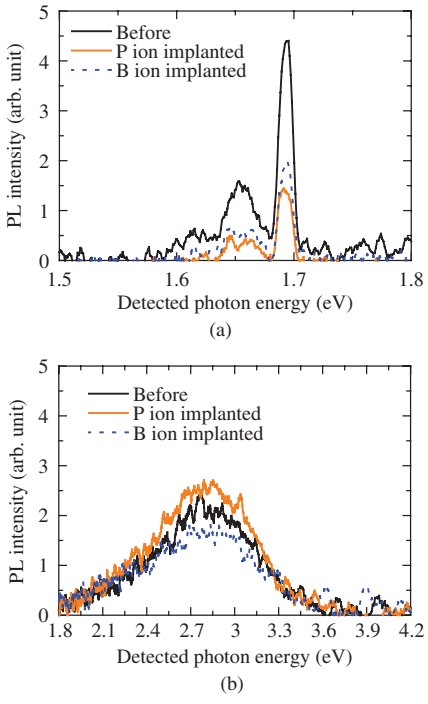


Fig. 1. PL spectra induced by the irradiation of 6.0-eV (a) and 5.0-eV (b) photons observed before and after the implantation of $P^+$ or $B^+$ ions at a dose of $10^{15}$ cm$^{-2}$

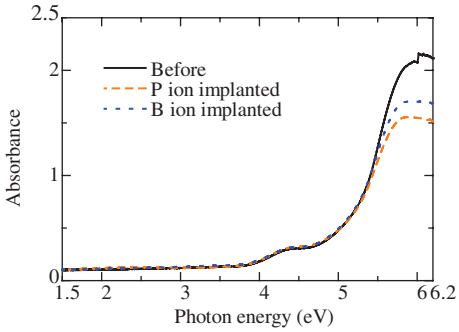


Fig. 2. Optical absorption spectra observed for $LaAlO_3$ samples with a thickness of ~0.5 mmat room temperature before and after the implantation of $P^+$ or $B^+$ ions at a dose of $10^{15}$ cm$^{-2}$

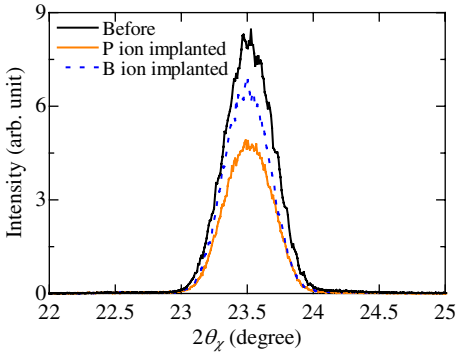


Fig. 3. In-plane XRD patterns observed before and after the implantation of $P^+$ or $B^+$ ions at a dose of $10^{15}$ cm$^{-2}$

Figure 3 shows the in-plane XRD spectra obtained from the surface area through which the ions with a dose of $10^{15}$ cm$^{-2}$ had passed. As indicated by the black solid curve, the unimplanted sample exhibits a peak at $2\theta_\chi = 23.5^\circ$, which corresponds to the diffraction from the (012) planes of crystalline $LaAlO_3$ [18]. The height of this peak decreases when the ions were implanted.

## 4. Discussion

First, the possibility of crystalline deformation is discussed based on the XRD results shown in Fig. 3. When the samples are hit by $P^+$ or $B^+$ ions, the ions seem to disrupt the crystal structure, since the XRD peak height decreases after ion implantation. This seems enough to conclude that the $LaAlO_3$ single crystal becomes at least partly amorphous when ions are implanted. However, such a conclusion cannot be drawn until we compare the thickness of the crystal where the ions had passed through and the one that could be properly analyzed by XRD.

When ions are implanted into a solid substance, they stop at a certain distance, which is called the projected range of the ions. Figure 4 shows projected ranges of $P^+$ and $B^+$ ions in $LaAlO_3$, calculated numerically by SRIM2011 [19]. The ranges are ~70 nm for $P^+$ ions and 160 nm for $B^+$ ions with an energy of 100 keV. Next, the depth measurable by in-plane XRD was estimated. Figure 5 shows the attenuation length of Cu K$\alpha$ X-rays estimated numerically [20]. When the grazing angle is $<0.34^\circ$, X-rays are reflected totally, resulting in a very short attenuation length, while the attenuation length increases rapidly when the angle exceeds $0.34^\circ$. This means that total reflection does not occur. Therefore, the grazing angle must be smaller than $0.34^\circ$ for in-plane XRD measurements. Therefore, the grazing angle was set at $0.32^\circ$ for measuring the XRD spectra shown in Fig. 3. Whatever the angle, the depth measurable by the in-plane XRD is less than 6 nm, which is far less than the projected range of 70 nm for $P^+$ ions or

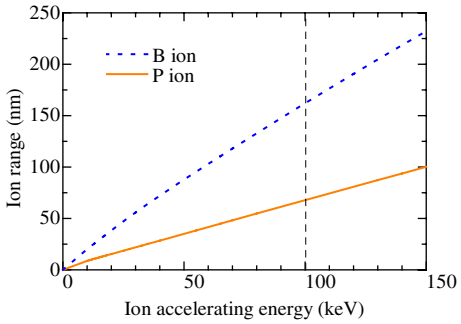


Fig. 4. Projected ranges of $P^+$ or $B^+$ ions in $LaAlO_3$

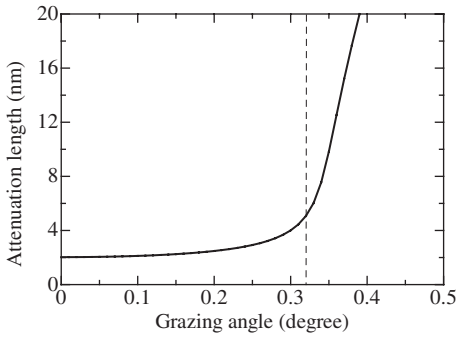


Fig. 5. Attenuation length of X-rays in $LaAlO_3$

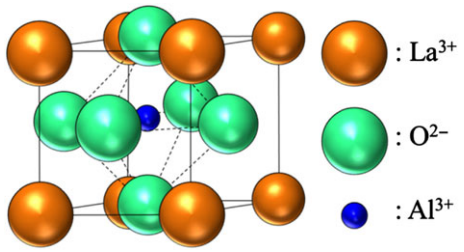


Fig. 6. Schematic diagram of the unit cell of perovskite $LaAlO_3$

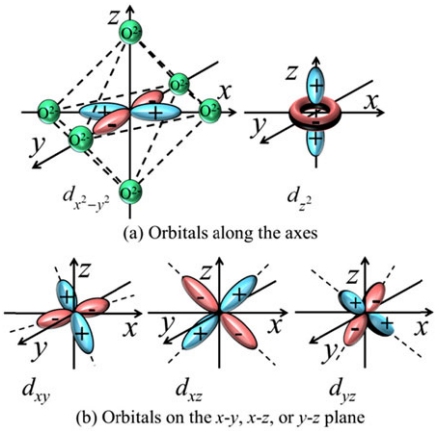


Fig. 7. Schematic diagrams of 3d orbitals in $Cr^{3+}$

160 nm for $B^+$ ions. On the other hand, the out-of-plane XRD is unsuitable, since its measurable depth is ∼1–6 μm, which is too large to obtain reliable information on the ion implantation effect. Therefore, we have to use an alternative suitable method.

From such a viewpoint, PL measurements were used as a method that could evaluate the crystallinity of the whole part in the sample where ions had passed through. As mentioned above, the PL spectra shown in Fig. 1(a) and 1(b) were, respectively, excited by photons with energies of 6.0 and 5.0 eV, and their peak energies range from about 1.6 to 3.6 eV. The optical absorption spectra shown in Fig. 2 obtained using samples ∼0.5 mm thickness strongly indicate that the incident photons with an energy of 5.0 or 6.0 eV can penetrate deep enough to cover the whole projected ranges of ions and that the emitted photons can go out of the sample to reach the detector.

As for the origins of PLs, the following assignment has been done. First, as for the three PL peaks at 1.62, 1.65 and 1.69 eV seen in Fig. 1(a), their spectral shapes are similar to those of the R-line luminescence of $Cr^{3+}$ in $LaAlO_3$ [16,21,22]. When $Al_2O_3$ contains Cr, it is called ruby, and when $Al_2O_3$ contains small amounts of Fe, it is sapphire. As indicated by these typical examples, Cr is generally present in materials containing aluminum, such as $LaAlO_3$ and $YAlO_3$ [23]. We have confirmed the presence of $Cr^{3+}$ in single crystals $LaAlO_3$ and $YAlO_3$ by electron spin resonance [23,24]. It is known that $LaAlO_3$ is a perovskite crystal with a structure shown in Fig. 6. Namely, $La^{3+}$ and $O^{2-}$ form a face-centered cube. A face-centered cube has a tetrahedral vacancy at its vertices and an octahedral vacancy at its center [18,22]. If $Al^{3+}$ occupies the latter central vacancy, the lattice becomes $LaAlO_3$. In the case of $YAlO_3$, $Cr^{3+}$ is known to expel $Al^{3+}$ and occupy easily the central octahedral vacancy as an impurity [21]. Therefore, it seems that $Cr^{3+}$ also occupies the octahedral vacancy by replacing $Al^{3+}$ in $LaAlO_3$ [22].

It is known that the electronic transition between the energy levels associated with the R-line luminescence of $Cr^{3+}$ is inherently forbidden. Nevertheless, the luminescence is observable due to the following mechanism. It has been reported that $Cr^{3+}$ forms an octahedral ligand field with $O^{2-}$ when the sample is crystalline and changes the degeneracy of its 3d orbital as a result of the Stark effect [22,25]. The 3d orbital generally shows fivefold degeneracy. However, in the octahedral ligand field shown in Fig. 7, two of the five 3d orbitals are along the directions toward $O^{2-}$ ions, while the three others are on the three planes that are perpendicular to the directions toward the $O^{2-}$ ions. Since electrons in the former two orbitals receive Coulombic repulsive forces induced by negatively charged $O^{2-}$, their energies increase. Compared with this, the energies of electrons in the latter three orbitals exhibit only a small increase. Namely, the fivefold degeneracy is split into two and three by the Stark effect. As a result, an excited level $^2E_g$ and a ground level $^4A_{2g}$ are generated. The R-line luminescence is induced by the transition of electrons from $^2E_g$ to $^4A_{2g}$ [25]. Therefore, the appearance of the three PLs at 1.62, 1.65 and 1.69 eV attributable to $Cr^{3+}$ indicates that the crystallinity of the sample is high.

We already confirmed that the above-mentioned three PLs did not appear in thin amorphous $LaAlO_3$ films made by spin-coating an alkoxide solution containing La and Al and that they appeared after the films had crystallized by thermal annealing at high temperatures [16]. As shown in Fig. 1(a), ion implantation decreases the intensities of the three PLs. This means that ion implantation reduces the crystallinity of the sample.

Secondly, the very broad PL spreading widely around 2.8 eV seen in Fig. 1(b) is due to oxygen vacancy [16]. This type of PL due to oxygen vacancy is known to appear in many oxides such as $YAlO_3$ [24], yttria-stabilized zirconia [26], ZnO [27], $Ta_2O_5$ [28], and $SiO_2$ [29,30], regardless of their crystallinity. For example, the PL is clearly observed in crystalline $LaAlO_3$ [16] and also in amorphous $SiO_2$ glasses deposited by a soot remelting method or by thermal oxidation [30]. Namely, the very little change in the intensity of the PL appearing in Fig. 1(b) and the significant decrease in the PL intensities shown in Fig. 1(a) are not contradictory but reasonable if we take the PL's origins into account.

To summarize all the results, the PLs that are observable only when the sample is crystalline become weak when $P^+$ or $B^+$ ions

are implanted. On the other hand, the PL due to oxygen vacancy, whose appearance is independent of the crystallinity, is not affected by the ion implantation. Therefore, the PL measurements consistently indicate that the crystallinity of single-crystal $LaAlO_3$ is degraded by the ion implantation.

Similar experiments have already been carried out for $YAlO_3$ [24,31], which is also a perovskite high-$k$ dielectric crystal similar to $LaAlO_3$ [21]. In contrast to the result of $LaAlO_3$ shown in Fig. 2, the optical band edge shifted toward a lower energy in the case of $YAlO_3$ [24,31], although the data is not shown here. This indicates that new localized electronic states were formed in the bandgap of $YAlO_3$ by the ion implantation. Namely, the change appearing in optical absorption near the absorption edge or at the photon energies close to $E_g$ is much more significant in $YAlO_3$ than in $LaAlO_3$. However, $E_g$ of $YAlO_3$ is ∼7.9 eV and is much higher than that of $LaAlO_3$. Regarding this, the absorption increase induced in $YAlO_3$ is significant only at energies higher than ∼6 eV. That is, if we pay attention to the same energy, e.g. 5 eV, the increase in optical absorption induced by the ion implantation is similar in $YAlO_3$ and $LaAlO_3$. Therefore, from an industrial viewpoint, the two high-$k$ dielectrics, i.e. $YAlO_3$ and $LaAlO_3$, have similar resistance against structural or crystallographic changes induced by the ion implantation.

## 5. Conclusion

Ions of $P^+$ or $B^+$ were implanted into single-crystal $LaAlO_3$, and their PL, optical absorption, and in-plane XRD spectra were measured. As a result, the following important results were obtained.

1. By the ion implantation, the optical absorption at energies beyond $E_g$ is decreased.
2. By the ion implantation, the intensity of the XRD (012) peak is decreased.
3. While the intensity of the PL at ∼2.8 eV due to oxygen vacancy does not change by the implantation, the intensities of three PL bands due to $Cr^{3+}$ at ∼1.65 eV become smaller by the ion implantation.

From points 2 and 3 above, it is clear that ion implantation degrades the crystallinity of $LaAlO_3$. This should be a matter of concern when $LaAlO_3$ is used as a high-$k$ gate dielectric of a device in which ions are implanted.

## Acknowledgments

Part of this research was supported by Power Academy and JSPS Grant 25 3090 for JSPS Fellows. It was also supported by Research Institute for Science and Engineering, Waseda University, through a grant from Mitsubishi Materials Corporation, 'Early Bird' grant for young researchers, and the ENEOS Research Encouragement Prize.

## References

(1) Yu SJ, Suzuki M, Ohki Y, Fujimaki M, Awazu K. Control of coupling ratio by proton implantation for directional coupler of planar-lightwave-circuit type. *Japanese Journal of Applied Physics* 2009; **48**:102405–1–102405–5.

(2) Fujimaki M, Ohki Y, Brebner JL, Roorda S. Fabrication of long-period optical fiber gratings by use of ion implantation. *Optics Letters* 2000; **25**:88–89.

(3) Yu SJ, Suzuki M, Ohki Y, Fujimaki M, Awazu K, Yamaguchi E, Okude S. Birefringence in optical fibers formed by proton implantation. *Nuclear Instruments and Methods in Physics Research Section B* 2007; **265**:490–494.

(4) Yu SJ, Ohki Y, Fujimaki M, Awazu K, Tominaga J, Sasa K, Komatsubara T. Reduction in polarization dependent loss of a planar lightwave circuit by ion-implantation-induced birefringence. *Nuclear Instruments and Methods in Physics Research Section B* 2008; **266**:4762–4765.

(5) Yu SJ, Ohki Y, Fujimaki M, Awazu K, Tominaga J. Optical fiber depolarizer using birefringence induced by proton implantation. *Japanese Journal of Applied Physics* 2009; **48**:032404–1–032404–3.

(6) Razavi B, Kuroda T. *Anarogu CMOS Syuuseki Kairo no Sekkei (Design of Analog CMOS Integrated Circuits) (in Japanese)*. Maruzen: Tokyo; 2003; 746 pp.

(7) Wilk GD, Wallace RM, Anthony JM. Hafnium and zirconium silicates for advanced gate dielectrics. *Journal of Applied Physics* 2000; **87**:484–492.

(8) Matsuoka M, Isotani S, Chubaci JFD, Miyake S, Setsuhara Y, Ogata K, Kuratani N. Influence of ion energy and arrival rate on x-ray crystallographic properties of thin ZrO$x$ films prepared on Si (111) substrate by ion-beam assisted deposition. *Journal of Applied Physics* 2000; **88**:3773–3775.

(9) Ito T, Maeda M, Nakamura K, Kato H, Ohki Y. Similarities in photoluminescence in hafnia and zirconia induced by ultraviolet photons. *Journal of Applied Physics* 2005; **97**:054104–1–054104–7.

(10) Kato H, Nango T, Miyagawa T, Katagiri T, Seol KS, Ohki Y. Plasma-enhanced chemical vapor deposition and characterization of high-permittivity hafnium and zirconium silicate films. *Journal of Applied Physics* 2002; **92**:1106–1111.

(11) Ito T, Kato H, Ohki Y. Mechanisms of several photoluminescence bands in hafnium and zirconium silicates induced by ultraviolet photons. *Journal of Applied Physics* 2006; **99**:094106–1–094106–9.

(12) Park BK, Park J, Cho M, Hwang CS, Oh K, Han Y, Yang DY. Interfacial reaction between chemically vapor-deposited $HfO_2$ thin films and a HF-cleaned Si substrate during film growth and postannealing. *Applied Physics Letters* 2002; **80**:2368–2370.

(13) Quevedo-Lopez M, El-Bouanani M, Addepalli S, Duggan JL, Gnade BE, Wallace RM, Visokay MR, Douglas M, Colombo L. Hafnium interdiffusion studies from hafnium silicate into silicon. *Applied Physics Letters* 2001; **79**:4192–4194.

(14) Suzuki M, Tomita M, Yamaguchi T, Koyama M. Ultra-thin $LaAlO_3$ gate dielectrics directly deposited. *Journal of Surface Science Society of Japan* 2007; **28**:22–27 (in Japanese).

(15) Hosoi T, Azumo S, Kashiwagi Y, Hosaka S, Nakamura R, Mitani S, Nakano Y, Asahara H, Nakamura T, Kimoto T, Shimura T, Watanabe H. Performance and reliability improvement in SiC power MOSFETs by implementing AlON high-$k$ gate dielectrics. *Proceedings of IEDM 2012 IEEE International Conference*, San Francisco, 2012; 7.4.1–7.4.4.

(16) Hirata E, Tamagawa K, Ohki Y. $Cr^{3+}$ impurities and photoluminescence in $LaAlO_3$. *Japanese Journal of Applied Physics* 2010; **49**:091102–1–091102–6.

(17) Robertson J. High dielectric constant gate oxides for metal oxide Si transistors. *Reports on Progress in Physics* 2006; **69**: 327–396.

(18) Lu CJ, Shen HM, Wang YN. Preparation and crystallization of $Pb(Zr_{0:95}Ti_{0:05})O_3$ thin films deposited by radio-frequency magnetron sputtering with a stoichiometric ceramic target. *Applied Physics A* 1998; **67**:253–258.

(19) Ziegler JF and Biersack JP. SRIM-2011 software package. http://www.srim.org/SRIM/SRIM2011.htm; 2011.

(20) Henke BL Gullikson EM, Davis JC. X-ray interactions: photoabsorption, scattering, transmission, and reflection at $E$ = 50-30,000 eV, $Z$ = 1-92. *Atomic Data and Nuclear Data Tables* 1993; **54**:181–342.

(21) Yamaga M, Takeuchi H, Han TPJ, Henderson B. Electron paramagnetic resonance and optical spectra of $Cr^{3+}$-doped $YAlO_3$. *Journal of Physi Condensed Matter* 1993; **5**:8097–8104.

(22) Heber J, Hellwege KH, Leutloff S, Platz W. Spectrum and energy levels of $Cr^{3+}$ ions and exchange-coupled $Cr^{3+}$ pairs in lanthanum aluminate. *Z. Physik* 1971; **246**:261–280.

(23) Yamasaka D, Horii Y, Morimoto T, Ohki Y. Roles of point defects in thermally enhanced generation and transfer of electrons and holes in $LaAlO_3$. *Japanese Journal of Applied Physics* 2013; **52**:071501–1–071501–5.

(24) Morimoto T, Horii Y, Inoue T, Kaneko S, Harima M, Ohki Y. Point defects in gate dielectrics $LaAlO_3$ and $YAlO_3$ for semiconductor devices—their varieties and structures, and the effects of ions,

photons, and thermal annealing -. *Journal of The Institute of Engineers on Electrical Discharges in Japan* 2014; **57**(**2**):3–12 (in Japanese).
(25) Champagnon B, Høg JH. Electric field effect on the optical absorption spectra of $V^{3+}$, $Cr^{3+}$ and $Co^{3+}$ in $\alpha$-$Al_2O_3$. *Chemical Physics Letters* 1977; **51**:429–432.
(26) Morimoto T, Takase M, Ito T, Kato H, Ohki Y. Defects in yttria-stabilized zirconia induced by irradiation of ultraviolet photons. *Japanese Journal of Applied Physics* 2008; **47**:6858–6862.
(27) Vanheusden K, Seager CH, Warren WL, Tallant DR, Voigt JA. Correlation between photoluminescence and oxygen vacancies in ZnO phosphors. *Applied Physics Letters* 1996; **68**:403–405.
(28) Zhu M, Zhang Z, Miao W. Intense photoluminescence from amorphous tantalum oxide films. *Applied Physics Letters* 2006; **89**: 021915–1–021915–3.
(29) Fujimaki M, Ohki Y, Nishikawa H. Energy states of Ge-doped $SiO_2$ glass estimated through absorption and photoluminescence. *Journal of Applied Physics* 1997; **81**:1042–1046.
(30) Nishikawa H, Watanabe E, Ito D, Ohki Y. Decay kinetics of the 4.4 eV photoluminescence associated with the two states of oxygen-deficient-type defect in amorphous $SiO_2$. *Physics Review Letters* 1994; **72**:2101–2104.
(31) Horii Y, Morimoto T, Ohki Y. Effect of ion implantation on the crystallinity of $YAlO_3$ single crystal. *UVSOR Activity Report* 2013; **40**:131.

**Masayuki Harima** (Student member) was born on July 19, 1991, in Saitama, Japan. He received the B.E. degree from Waseda University, Japan, in 2014, and is currently pursuing graduate studies there.

**Takaaki Morimoto** (Non-member) was born on July 27, 1982, in Tokyo, Japan. He received the M.E. degree in 2008 from Waseda University, Japan, and is currently pursuing the Ph.D. degree there. From 2008 to 2012, he was with Hitachi Central Research Laboratory, engaged in research on analog electronic circuits. His current research interests include high-permittivity insulating materials for semiconductors.

**Yoshimichi Ohki** (Fellow) is a Professor with the Department of Electrical Engineering and Bioscience and Research Institute for Materials Science and Technology, Waseda University, Japan. He is also an Honorary Professor with Xian Jiaotong University, China. He was a Visiting Scientist at the Massachusetts Institute of Technology, USA, from 1982 to 1984. He is a recipient of the Forster, Whitehead, and Ieda Awards from IEEE-DEIS, the Outstanding Achievement Award, the Technical Development Award, and two Best Paper Awards from IEE Japan, among others. His major research interests include various organic and inorganic dielectrics, e.g. those used in optical fibers and power cables.